

# Prediction of sustained production casing pressure and casing design for shale gas horizontal wells



Fei Yin\*, Deli Gao

MOE Key Laboratory of Petroleum Engineering, China University of Petroleum, China

## ARTICLE INFO

### Article history:

Received 16 February 2015

Received in revised form

19 April 2015

Accepted 30 April 2015

Available online 15 May 2015

### Keywords:

Shale gas

Horizontal well

Hydraulic fracturing

Sustained casing pressure

Casing design

## ABSTRACT

Casing failure in shale gas horizontal wells hinders the efficient development of shale gas. The sustained casing pressure is the main failure mechanism, while the current analytic methods are not fit to shale gas horizontal wells. Hydraulic fracturing causes well temperature change, so the temperature distribution of horizontal well section is calculated based on heat transfer theory. According to thermoelasticity, the formula of annular volume change under the synergy of temperature and pressure is deduced. By substituting the temperature distribution and annular volume change into the prediction model, the sustained production casing pressure in horizontal wells is obtained. For the work condition of production casings in shale gas horizontal wells, an improved method of casing design is proposed. Results indicate that the horizontal well temperature increases with the distance increase from well axis in the pattern of line-parabola. The thermoelastic deformations of production casing and surrounding rock change the annular volume observably. The sustained production casing pressure displays a quadratic polynomial increase with well temperature. The hydraulic fracturing pressure and sustained casing pressure should be involved to design the production casing in shale gas horizontal wells. The research provides the prediction method of sustained production casing pressure in horizontal wells. The proposed casing design method for shale gas horizontal wells ensures well integrity.

© 2015 Elsevier B.V. All rights reserved.

## 1. Introduction

The shale gas reservoir is endowed with the physical characteristics of low porosity and low permeability. Horizontal drilling and multistage hydraulic fracturing are the key technologies to get industrial gas flow (Liu et al., 2012; Nassir et al., 2014; Frash et al., 2014). Multistage fracturing after cementing casing is a common well completion method. The process includes: running in production casing, cementing, hydraulic fracturing after pumping bridge plug and perforation, drilling bridge plug by using coiled tubing (Aaron et al., 2006; Zhao et al., 2012). Hydraulic fracturing makes the load of production casing more complex and causes casing failure potentially (Yu et al., 2014). Casing deformation induces obstruction in the operations of pumping or drilling bridge plug. For example, in Changning-Weiyuan demonstration zone of shale gas, there were 11 vertical wells and 12 horizontal wells that have been fractured, but 2 vertical wells and 8 horizontal wells occurred casing

deformation. Casing steel grade is enhanced from P-110 to Q-125, then to V-140 (Feng et al., 2014). Casing failure has increased operation cost and hindered efficient development of shale gas. There are more than ten kinds of potential factors, including internal pressure, external pressure, bending, perforation, temperature, microseism and shale rock movement, etc.

Well temperature changes during the process of multistage hydraulic fracturing. So, sustained casing pressure is judged as one of main failure mechanisms after screening analysis. Due to irregular wellbore, long horizontal interval, decenter casing in wellbore and inferior compatibility between cement slurry and oil-based drilling fluid, it is difficult to implement efficient displacement. Furthermore, large-scale multistage fracturing damages cement sheath and causes annular channeling potentially (Wu et al., 2012; Zhou 2013). According to oilfield data, sustained casing pressure is detected at wellhead in some shale wells after fracturing.

The sustained casing pressure in HPHT wells has attracted much attention. Theoretical models of predicting sustained casing pressure have been proposed by some scholars (Adams, 1991; Pattillo et al., 2004; Oudeman and Kerem, 2006; Rocha et al., 2014).

\* Corresponding author.

E-mail address: [yinfei999@163.com](mailto:yinfei999@163.com) (F. Yin).

These models are established by calculating thermal expansion of fluid and volume change of casing annulus. Roger et al. (2003) and Neil et al. (2008) measured the sustained casing pressure in laboratory or in oilfield by wireless acoustic gauges. The measured value is consistent with the predicted value. However, the annular pressure between production casing and wellbore in horizontal wells has not been studied or measured. To address this issue, a new prediction model of sustained production casing pressure is established and casing design method for shale gas horizontal wells is proposed. Firstly, the temperature distribution of horizontal well section is calculated. Afterward, the volume change under the synergy of temperature and pressure is calculated based on thermoelasticity. At last, sustained production casing pressure can be predicted accurately. Furthermore, the design method of production casing is proposed for shale gas horizontal wells and it is demonstrated to be reasonable by oilfield application.

## 2. Temperature distribution of horizontal well section

In drilling engineering, well temperature is low when drilling fluid is circulating. After drilling fluid circulation, the heat of far high-temperature formation transmits to the well, so well temperature increases (Toni et al., 2003; Yang et al., 2013). During the operation of hydraulic fracturing in shale gas horizontal wells, well temperature will also change with the conversion from fracturing to stop injection. Determining the temperature distribution of well and surrounding rock is the precondition of predicating sustained casing pressure.

In order to establish the calculation models of temperature field and sustained casing pressure, the following assumptions are made:

- The poor cementing quality and hydraulic fracturing lead to partial annulus at the outside of production casing (Fig. 1). Multistage fracturing horizontal wells should be analyzed for fluid contraction even where the annulus is contact with a reservoir (Jonathan et al., 2013).
- The cement sheath is very thin and its mechanical and thermal properties are similar to those of surrounding rock (Nabipour et al., 2010), so the cement sheath can be considered as a part of surrounding rock.
- In the horizontal well section, the temperature field of well and surrounding rock is axisymmetric.
- The temperatures at the inner wall of production casing and outer margin of surrounding rock are constant. And there is only heat conduction among casing, annulus and surrounding rock.
- The inner pressure of casing and in-situ stress are constant.

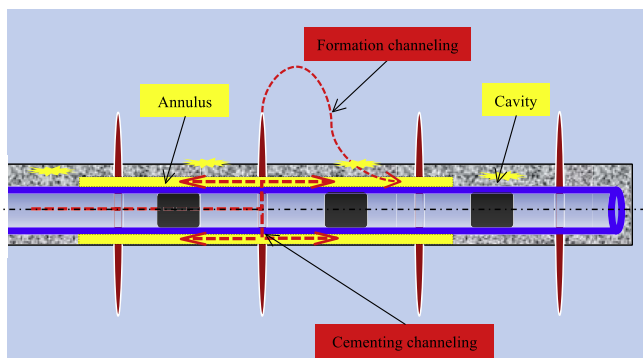


Fig. 1. Diagram of multistage fracturing horizontal well and partial annulus.

The schematic diagram of heat conduction among casing, annulus and surrounding rock is shown in Fig. 2.

In polar coordinate, the differential equation of steady heat conduction of cylinder (Ana et al., 2004) is:

$$\frac{d^2T}{dr^2} + \frac{1}{r} \frac{dT}{dr} = 0 \quad (1)$$

According to integral and boundary conditions, the temperature field is solved:

$$T(r) = T_i - (T_i - T_o) \ln \frac{r}{r_i} / \ln \frac{r_o}{r_i} \quad (2)$$

Based on Fourier law, the heat flux per unit length is:

$$\Phi = \frac{T_i - T_o}{\frac{1}{2\pi\lambda} \ln \frac{r_o}{r_i}} \quad (3)$$

For the combined structure of casing, annular fluid and surrounding rock, the heat flux per unit length is:

$$\Phi = \frac{T_4 - T_1}{\frac{1}{2\pi\lambda_1} \ln \frac{b}{a} + \frac{1}{2\pi\lambda_2} \ln \frac{c}{b} + \frac{1}{2\pi\lambda_3} \ln \frac{d}{c}} \quad (4)$$

The temperatures at casing outer wall and wellbore are solved:

$$\begin{cases} T_2 = T_4 - \Phi \left( \frac{1}{2\pi\lambda_3} \ln \frac{d}{c} + \frac{1}{2\pi\lambda_2} \ln \frac{c}{b} \right) \\ T_3 = T_4 - \Phi \frac{1}{2\pi\lambda_3} \ln \frac{d}{c} \end{cases} \quad (5)$$

By substituting Eq. (5) into Eq. (2), the temperature fields of casing, annulus and surrounding rock are solved:

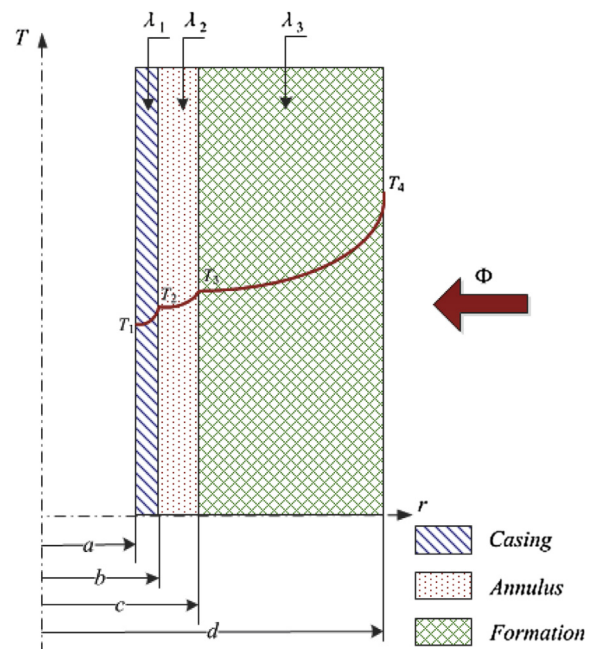


Fig. 2. Schematic diagram of heat conduction among casing, annulus and surrounding rock.

$$\begin{cases} T_c(r) = T_1 - (T_1 - T_2) \ln \frac{r}{a} / \ln \frac{b}{a} \\ T_{ann}(r) = T_2 - (T_2 - T_3) \ln \frac{r}{b} / \ln \frac{c}{b} \\ T_f(r) = T_3 - (T_3 - T_4) \ln \frac{r}{c} / \ln \frac{d}{c} \end{cases} \quad (6)$$

### 3. Calculation of sustained production casing pressure

#### 3.1. Model of sustained casing pressure

Sustained casing pressure is a function of annular temperature, annular volume and fluid mass (Oudeman and Kerem, 2006), and it can be expressed as:

$$p = p(T, V_{ann}, m) \quad (7)$$

Its partial differential is:

$$\Delta p = \left( \frac{\partial p}{\partial T} \right) \Delta T + \left( \frac{\partial p}{\partial V_{ann}} \right) \Delta V_{ann} + \left( \frac{\partial p}{\partial m} \right) \Delta m \quad (8)$$

Coefficient of thermal expansion is the change of unit volume induced by unit temperature change. Its expression is:

$$\alpha_l = \frac{\Delta V}{V \cdot \Delta T} \quad (9)$$

Coefficient of compressibility is the change of unit volume induced by unit pressure change. Its expression is:

$$\kappa_T = \frac{\Delta V}{V \cdot \Delta p} \quad (10)$$

By substituting Eqs. (9) and (10) into Eq. (8), the sustained casing pressure can be obtained.

$$\Delta p = \frac{\alpha_l}{\kappa_T} \cdot \Delta T - \frac{1}{\kappa_T \cdot V_{ann}} \cdot \Delta V_{ann} + \frac{1}{\kappa_T \cdot V_l} \cdot \Delta V_l \quad (11)$$

The sustained casing pressure is composed of three parts. They are the pressure induced by fluid thermal expansion, the pressure induced by annular volume change and the pressure induced by fluid influx or leakage. In the sealed annulus, the pressure induced by fluid influx or leakage is zero. The pressure induced by fluid thermal expansion plays a dominant role, but the annular volume change affects the annular pressure significantly.

#### 3.2. Calculation of annular volume change

Determining the annular volume change is the key of predicating sustained casing pressure accurately. It is difficult to determine the annular volume because annular volume, temperature and pressure are coupling interaction. The annular volume change includes: the thermal expansions of casing and surrounding rock when temperature increases, and the deformations of casing and surrounding rock when annular pressure changes.

The production casing, annulus and surrounding rock form a combined cylindrical structure. It can be simplified into a plane strain problem, and the mechanical model is shown in Fig. 3.

By adopting thermoelasticity, the formula of annular volume change under the synergy of temperature and pressure can be deduced. The thermoelastic behavior of production casing will be analyzed firstly as follows.

The equilibrium equation is:

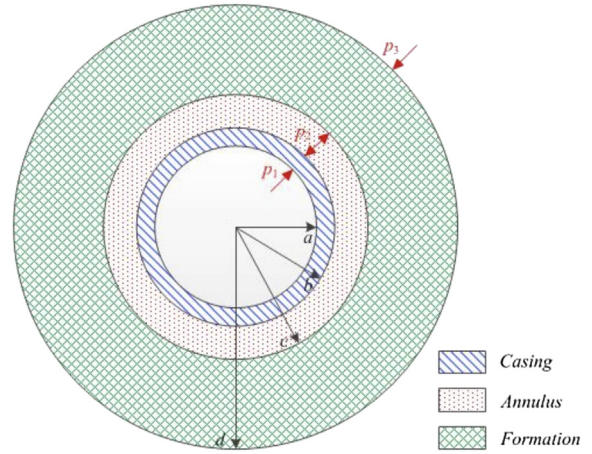


Fig. 3. The mechanical model of production casing, annulus and surrounding rock.

$$\frac{d\sigma_r}{dr} + \frac{\sigma_r - \sigma_\theta}{r} = 0 \quad (12)$$

The geometric equation is:

$$\begin{cases} \epsilon_r = \frac{du}{dr} \\ \epsilon_\theta = \frac{u}{r} \end{cases} \quad (13)$$

The physical equation is:

$$\begin{cases} \epsilon_r = \frac{1}{E} [\sigma_r - \nu(\sigma_\theta + \sigma_z)] + \alpha \Delta T \\ \epsilon_\theta = \frac{1}{E} [\sigma_\theta - \nu(\sigma_r + \sigma_z)] + \alpha \Delta T \\ \epsilon_z = \frac{1}{E} [\sigma_z - \nu(\sigma_r + \sigma_\theta)] + \alpha \Delta T \end{cases} \quad (14)$$

For the plane strain, the axial displacement is zero:

$$\epsilon_z = 0 \quad (15)$$

By synthesizing the above fundamental equations, the radial displacement and stress components are solved (Timoshenko and Goodier, 1970):

$$\begin{cases} u = \frac{1+\nu}{1-\nu} \alpha \frac{1}{r} \int_a^r \Delta T r dr + C_1 r + \frac{C_2}{r} \\ \sigma_r = -\frac{\alpha E}{1-\nu} \frac{1}{r^2} \int_a^r \Delta T r dr + \frac{E}{1+\nu} \left( \frac{C_1}{1-2\nu} - \frac{C_2}{r^2} \right) \\ \sigma_\theta = \frac{\alpha E}{1-\nu} \frac{1}{r^2} \int_a^r \Delta T r dr - \frac{\alpha E \Delta T}{1-\nu} + \frac{E}{1+\nu} \left( \frac{C_1}{1-2\nu} + \frac{C_2}{r^2} \right) \\ \sigma_z = -\frac{\alpha E \Delta T}{1-\nu} + \frac{2\nu E C_1}{(1+\nu)(1-2\nu)} \end{cases} \quad (16)$$

According to the boundary conditions of production casing:

$$\begin{cases} (\sigma_r)_{r=a} = -p_1 \\ (\sigma_r)_{r=b} = -p_2 \end{cases} \quad (17)$$

The parameters of  $C_1$  and  $C_2$  are obtained by substituting Eq. (17) into Eq. (16):

$$\begin{cases} C_1 = \frac{(1+\nu)(1-2\nu)}{E} \frac{a^2 b^2}{b^2 - a^2} \left( \frac{p_1}{b^2} - \frac{p_2}{a^2} \right) + \frac{(1+\nu)(1-2\nu)}{1-\nu} \alpha \frac{1}{b^2 - a^2} \int_a^b \Delta T r dr \\ C_2 = \frac{1+\nu}{E} \frac{a^2 b^2}{b^2 - a^2} (p_1 - p_2) + \frac{1+\nu}{1-\nu} \alpha \frac{a^2}{b^2 - a^2} \int_a^b \Delta T r dr \end{cases} \quad (18)$$

So, the analytic solutions of the radial displacement and stress components are obtained. Thereinto, the radial displacement of production casing is:

$$\begin{aligned} u = & \frac{1+\nu}{E} \left[ \frac{a^2 b^2 + (1-2\nu)a^2 r^2}{(b^2 - a^2)r} p_1 - \frac{a^2 b^2 + (1-2\nu)b^2 r^2}{(b^2 - a^2)r} p_2 \right] \\ & + \frac{1+\nu}{1-\nu} \alpha \frac{1}{r} \int_a^r \Delta T r dr + \frac{(1+\nu)(1-2\nu)}{1-\nu} \alpha \frac{r}{b^2 - a^2} \int_a^b \Delta T r dr \\ & + \frac{1+\nu}{1-\nu} \alpha \frac{a^2}{(b^2 - a^2)r} \int_a^b \Delta T r dr \end{aligned} \quad (19)$$

If annular temperature increases by  $\Delta T_c$  and the outer pressure of production casing (sustained casing pressure) increases by  $\Delta p$ , the radial displacement of production casing's outside wall is:

$$u_b = -\frac{1+\nu}{E} \frac{a^2 b + (1-2\nu)b^3}{b^2 - a^2} \Delta p + (1+\nu) \alpha \frac{2b}{b^2 - a^2} \int_a^b \Delta T_c r dr \quad (20)$$

Thus, the annular volume change caused by the thermoelastic deformation of production casing is:

$$\Delta V_{\text{anni}} = \pi [b^2 - (b + u_b)^2] L_{\text{anno}} \quad (21)$$

It indicates that the thermal expansion of production casing decreases the annular volume, and the mechanical compression of production casing increases the annular volume.

Take surrounding rock as another study object. According to the solution process of production casing, the deformation of surrounding rock can be solved too. When annular temperature increases by  $\Delta T_f$  and sustained casing pressure increases by  $\Delta p$ , the radial displacement of wellbore is:

$$u_c = \frac{1+\nu_f}{E_f} \frac{cd^2 + (1-2\nu_f)c^3}{d^2 - c^2} \Delta p + (1+\nu_f) \alpha_f \frac{2c}{d^2 - c^2} \int_c^d \Delta T_f r dr \quad (22)$$

Thus, the annular volume change caused by the thermoelastic deformation of surrounding rock is:

$$\Delta V_{\text{anno}} = \pi [(c + u_c)^2 - c^2] L_{\text{anno}} \quad (23)$$

The annular volume change is equal to the sum of annular volume changes caused by the deformations of production casing and surrounding rock.

$$\Delta V_{\text{ann}} = \Delta V_{\text{anni}} + \Delta V_{\text{anno}} \quad (24)$$

The initial annular volume is:

$$V_{\text{ann}} = \pi (c^2 - b^2) L_{\text{anno}} \quad (25)$$

The value of sustained casing pressure can be calculated by iteration method. The iterative process is: a series of initial values  $\Delta p(i)$  are set and substitute them into Eq. (20) and Eq. (22); then substitute Eqs. (21), (23)–(25) into Eq. (11), so a new value  $\Delta p(i+1)$  is obtained ( $i$  represents iterative times); if  $\Delta p(i+1)$  is same or extremely similar to  $\Delta p(i)$ , this result is the value of sustained casing pressure. This solution can be performed in computer programs.

The sustained production casing pressure in horizontal wells can be predicated by this model. This model takes fluid thermal expansion and the annular volume change caused by the thermoelastic deformations of production casing and surrounding rock into account, so it is more accurate.

#### 4. Case analysis

The H3-1 well is one of shale gas horizontal wells in the Changning-Weiyuan national demonstration zone of shale gas. According to drilling engineering design, the wellbore size in reservoir is 168.28 mm, the outer diameter of P-110 production casing is 127 mm and the wall thickness is 12.14 mm. After drilling and cementing, the  $\Phi$  100 mm drilling bit was used to drill cement plug. Before hydraulic fracturing, the  $\Phi$  96 mm gauge ring was used to make a wiper trip. There is no obstruction in these operations. But, when coiled tubing was used to drill bridge plug after hydraulic fracturing, the  $\Phi$  96–86 mm milling shoes cannot pass through at well depth of 2924 m. Furthermore, moulage was seen by lead print at this location and it indicated that production casing deformed.

The fracturing operation is divided into 12 intervals. The well temperature changes about 20 times. The well temperature is 293 K when fracturing, while the well temperature increases to 333 K after fracturing. The temperature of surrounding rock's outer margin is 372 K.

The heat conductivity coefficient of casing is 30 W/(m·K). The heat conductivity coefficient of fluid is 1.75 W/(m·K). The heat conductivity coefficient of surrounding rock is 0.1 W/(m·K) (Shan et al., 2004). By calculation, the temperature distribution of horizontal well section is shown in Fig. 4. The temperature of horizontal well is varying with the distance from well axis in the pattern of line-parabola.

The elastic modulus of shale rock in Longmaxi group is  $3.2 \times 10^4$  MPa, Poisson's ratio is 0.18 (Yuan et al., 2013), and the coefficient of thermal expansion is  $5.899 \times 10^{-5} \text{ }^\circ\text{C}^{-1}$ . The elastic modulus of casing is  $2.06 \times 10^5$  MPa, Poisson's ratio is 0.3, and the coefficient of thermal expansion is  $1.20 \times 10^{-5} \text{ }^\circ\text{C}^{-1}$ . The coefficients of thermal expansion and compressibility of fluid under

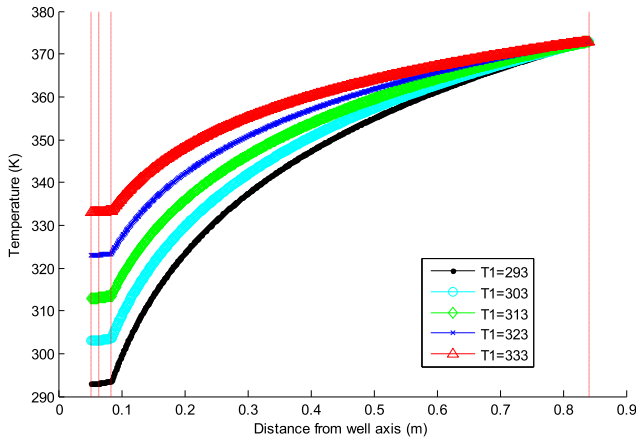


Fig. 4. The temperature distribution of horizontal well section.

arbitrary temperature can be obtained by the method of interpolation (Yin and Gao, 2014). Based on the above calculation model of sustained production casing pressure, the sustained production casing pressure in H3-1 well is shown in Fig. 5. The sustained production casing pressure displays a quadratic polynomial increase with well temperature after fracturing.

The values of sustained production casing pressure are listed in Table 1. The annular volume change ( $\Delta V_{ann}$ ) can make the sustained production casing pressure decrease by 38.2% averagely. The sustained production casing pressures is 21.6 MPa when well temperature increases by 40 K after fracturing.

In this shale gas field, the density of drilling fluid used in the reservoir is  $2.2 \text{ g/cm}^3$ . According to the conventional standard of casing design, the external pressure of production casing is 53.4 MPa and the safety factor of collapse strength is 2.5. But, casing failure indicates that the casing design standard is not suitable for shale gas horizontal wells after hydraulic fracturing. For shale gas horizontal wells undergoing hydraulic fracturing, the most dangerous condition of production casing is: fracturing fluid flows into the annulus of production casing then is sealed, and the sustained casing pressure occurs after fracturing. Due to the potential scratches of production casing during downhole operations, the designed safety factor of collapse strength is recommended as the upper limit 1.125.

The maximum external pressure of production casing in shale gas horizontal wells undergoing hydraulic fracturing can be calculated by this formula.

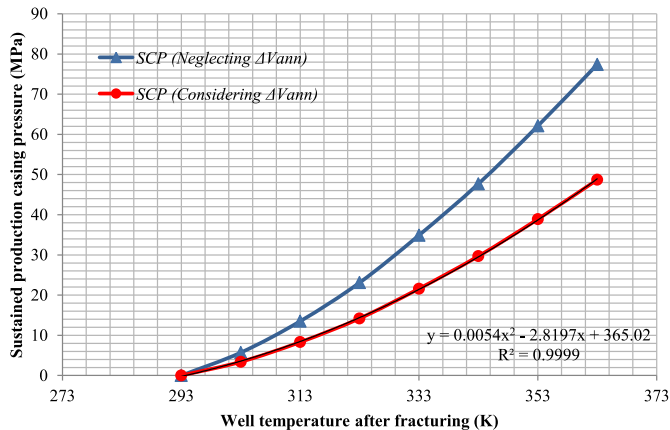


Fig. 5. The sustained production casing pressure versus well temperature.

Table 1  
The sustained production casing pressure.

Well temperature increase (K)	Sustained production casing pressure (MPa)		Deviation
	Neglecting $\Delta V_{ann}$	Considering $\Delta V_{ann}$	
10	5.7	3.4	40.4%
20	13.5	8.3	38.5%
30	23.1	14.2	38.5%
40	34.9	21.6	38.1%
50	47.7	29.7	37.7%
60	62.1	38.9	37.4%
70	77.4	48.7	37.1%

$$p_{frc} = p_{pump} + 0.00981 [\rho_{frc} - (1 - k_m)\rho_w] h_{hor} + \Delta p \quad (26)$$

In this example, the potential maximum external pressure of production casing is:  $p_{frc} = 87 + 17 + 21.6 = 125.6 \text{ MPa}$ . Based on the new method of casing design, the designed external pressure of production casing should be 141.3 MPa. According to this method, the  $\Phi 127 \text{ mm}$  production casing with wall thickness 12.14 mm and steel grade TP140V is recommended. This kind of casing hasn't been found to deform or fail. The parameters and failure situation of production casings in the shale gas field can be found in the appendix. Oilfield application demonstrates this design method is reliable.

### 5. Conclusions

- (1) Casing failure occurs frequently in shale gas horizontal wells. There are many inducements, but the sustained casing pressure associated with fracturing is considered to be the main failure mechanism.
- (2) The sustained casing pressure is affected by fluid thermal expansion, annular volume change and fluid influx or leakage. The thermoelastic deformations of production casing and surrounding rock increase the annular volume. It makes the annular pressure induced by fluid thermal expansion decrease by 38.2% averagely.
- (3) The sustained production casing pressure displays quadratic polynomial increase with well temperature after fracturing in horizontal wells.
- (4) The most dangerous work condition of production casing in shale gas horizontal wells is the fracturing fluid flowing into the annulus then being sealed, and the temperature change adding the sustained casing pressure.
- (5) The new design method of production casing can ensure the integrity of shale gas horizontal wells. It is demonstrated to be reliable by oilfield application.

### Acknowledgments

The authors gratefully acknowledge the financial support of the Natural Science Foundation of China (NSFC, 51221003). This research was also supported by the other projects (Grant numbers: 2014 A-4214, 2010CB226703, 2011ZX05009).

### Nomenclature

- $a$  inside radius of casing, m
- $b$  outside radius of casing, m
- $c$  radius of wellbore, m
- $d$  radius of surrounding rock, m
- $r$  radius of cylinder, m
- $r_i$  inside radius of cylinder, m

$r_o$	outside radius of cylinder, m	$\nu_f$	Poisson's ratio of surrounding rock
$L_{ann}$	length of annulus, m	$m$	mass of fluid in annulus, kg
$h_{hor}$	vertical depth of horizontal well section, m	$\rho_{frc}$	density of fracturing fluid, g/cm <sup>3</sup>
$u$	radial displacement, m	$\rho_w$	density of completion fluid, g/cm <sup>3</sup>
$u_b$	radial displacement of casing, m	$k_m$	empty coefficient of casing
$u_c$	radial displacement of wellbore, m		
$p$	pressure, MPa		
$p_1$	internal pressure of casing, MPa		
$p_2$	annular pressure, MPa		
$p_3$	in-situ stress, MPa		
$\Delta p$	sustained casing pressure, MPa		
$p_{frc}$	maximum external pressure of production casing, MPa		
$p_{pump}$	pump pressure when fracturing, MPa		
$T$	temperature, °C		
$T_i$	temperature of cylinder inside wall, °C		
$T_o$	temperature of cylinder outside wall, °C		

### Appendix. Production casing data in Changning-Weiyuan shale gas field

The parameters and failure situation of production casings in Changning-Weiyuan shale gas field are shown in Table 2. Casing failure accidents occur frequently in this field when employing the casings according to the conventional standard of casing design. The production casings designed by sustained production casing pressure are undamaged.

**Table 2**  
The parameters and failure situation of production casings.

Development stage	Well number	Reservoir layer	Casing OD (mm)	Wall thickness (mm)	Burst strength (MPa)	Collapse strength (MPa)	Failure situation
1	Wei 201-H1	Longmaxi	139.7	9.17	75.3	69	Casing deformation
	Wei 201-H3	Qiongzhusi	139.7	9.17	71.6/77.7	87.2/88.5	Casing deformation
	Ning 201-H1	Longmaxi	139.7	9.17	85.31/96.94	76.5/100.2	Casing deformation
2	Wei 204	Longmaxi	139.7	12.7	154	172.4	Integrity
	Wei 205	Longmaxi	127	12.14	161.5	149.2	Integrity
3	Ning H3-1	Longmaxi	127	12.14	102.5	131.1	Casing deformation
	Ning H3-2	Longmaxi	127	12.14	102.5	131.1	Casing deformation
	Ning H3-3	Longmaxi	127	12.14	102.5	131.1	Integrity
	Ning H2-1	Longmaxi	127	12.14	102.5	131.1	Casing deformation
	Ning H2-2	Longmaxi	127	12.14	102.5	131.1	Integrity
	Ning H2-3	Longmaxi	127	12.14	102.5	131.1	Casing deformation
	Ning H2-4	Longmaxi	127	12.14	102.5	131.1	Casing deformation

$T_1, T_2, T_3, T_4$  temperatures of casing inside wall, casing outside wall, annulus outside wall, surrounding rock, °C

$T(r)$  temperature distribution, °C

$T_c(r), T_{ann}(r), T_f(r)$  temperature distributions of casing, annulus, surrounding rock, °C

$\Delta T$  temperature change, °C

$V$  volume, m<sup>3</sup>

$V_{ann}$  volume of annulus, m<sup>3</sup>

$V_f$  volume of fluid, m<sup>3</sup>

$\Delta V$  volume change, m<sup>3</sup>

$\Delta V_{ann}$  volume change of annulus, m<sup>3</sup>

$\Delta V_{anni}$  volume change of annulus induced by casing deformation, m<sup>3</sup>

$\Delta V_{anno}$  volume change of annulus induced by surrounding rock deformation, m<sup>3</sup>

$\Delta V_f$  volume change of fluid in annulus, m<sup>3</sup>

$\Phi$  heat flux per unit length, W/m

$\lambda$  heat conductivity coefficient, W/(m·K)

$\lambda_1, \lambda_2, \lambda_3$  heat conductivity coefficients of casing, annular fluid, surrounding rock, W/(m·K)

$\sigma_r, \sigma_\theta, \sigma_z$  radial stress, circumferential stress, axial stress, MPa

$\varepsilon_r, \varepsilon_\theta, \varepsilon_z$  radial strain, circumferential strain, axial strain

$\alpha$  coefficient of thermal expansion of casing, °C<sup>-1</sup>

$\alpha_f$  coefficient of thermal expansion of surrounding rock, °C<sup>-1</sup>

$\alpha_l$  coefficient of thermal expansion of fluid, °C<sup>-1</sup>

$\kappa_T$  coefficient of compressibility, MPa<sup>-1</sup>

$E$  elastic modulus of casing, MPa

$E_f$  elastic modulus of surrounding rock, MPa

$\nu$  Poisson's ratio of casing

### References

- Aaron, Allen Ketter, Daniels, John Leonard, Heinze, James R., et al., 2006. A field study optimizing completion strategies for fracture initiation in Barnett shale horizontal wells. In: Paper SPE 103232 Presented at SPE Annual Technical Conference and Exhibition, Texas, USA, 24–27 September.
- Adams, A., 1991. How to design for annulus fluid heat-up. In: Paper 22871 Presented at the SPE Annual Technical Conference and Exhibition, Dallas, 6–9 October.
- Ana, Maria Bianchi, Yves, Fautrelle, Jacqueline, Etay, 2004. Transferts thermiques. Presses polytechniques et universitaires romandes. Lausanne, Agence universitaire de la francophonie, Montreal.
- Feng, Yaorong, Han, Lihong, Zhang, Fuxiang, et al., 2014. Research progress and prospect of oil and gas well tubing string integrity technology. Nat. Gas. Ind. 34 (11), 73–81.
- Frash, Luke P., Gutierrez, Marte, Hampton, Jesse, 2014. Laboratory-scale-model testing of well stimulation by use of mechanical-impulse hydraulic fracturing. SPE J. 1–14. SPE-173186-PA.
- Jonathan, Bellarby, Sara Sparre, Kofoed, Franz, Marketz, 2013. Annular pressure build-up analysis and methodology with examples from multfrac horizontal wells and HPHT reservoirs. In: Paper SPE 163557 Presented at the SPE/IADC Drilling Conference and Exhibition, Amsterdam, The Netherlands, 5–7 March.
- Liu, Wei, Tao, Qian, Ding, Shidong, 2012. Difficulties and countermeasures for cementing technology of shale gas horizontal well. Oil Drill. Prod. Technol. 34 (3), 40–43.
- Nabipour, A., Joodi, B., Sarmadivaleh, M., 2010. Finite element simulation of downhole stresses in deep gas wells cements. In: Paper SPE 132156 Presented at SPE Deep Gas Conference and Exhibition, Manama, Bahrain, 24–26 January.
- Nassir, M., Settari, A., Wan, R., 2014. Prediction of stimulated reservoir volume and optimization of fracturing in tight gas and shale with a fully elasto-plastic coupled geomechanical model. SPE J. 10, 771–785. SPE-163814-PA.
- Neil, Sultan, Jean, Baptiste Faget, Mikkel, Fjeldheim, et al., 2008. Real-time casing annulus pressure monitoring in a subsea HPHT exploration well. In: Paper OTC 19286 Presented at the Offshore Technology Conference, Houston, Texas, 5–8 May.
- Oudeman, P., Kerem, M., 2006. Transient behavior of annular pressure buildup in HP/HT wells. SPE Drill. Complet. 21 (4), 234–241. SPE-88735-PA.
- Pattillo, P.D., Cocales, B.W., Morey, S.C., 2004. Analysis of an annular pressure buildup failure during drill ahead. In: Paper SPE 89775 Presented at the SPE Annual Technical Conference and Exhibition, Houston, Texas, 26–29

- September.
- Rocha, Valadez T., Hasan, A.R., Mannan, S., et al., 2014. Assessing wellbore integrity in sustained casing pressure annulus. *SPE Drill. Complet.* 3, 131–138. SPE-169814-PA.
- Roger, Williamson, Wayne, Sanders, Troy, Jakabosky, et al., 2003. Control of contained annulus fluid pressure buildup. In: Paper SPE 79875 Presented at the SPE/IADC Drilling Conference, Amsterdam, The Netherlands, 19–21 February.
- Shan, Xuejun, Zhang, Shicheng, Wang, Wenxiong, et al., 2004. The factors influencing the wellbore temperature in heavy oil production. *Pet. Explor. Dev.* 31 (3), 136–139.
- Timoshenko, S.P., Goodier, J.N., 1970. *Theory of Elasticity*, third ed. McGraw Hill Education.
- Toni, Loder, Evans, Jason H., Griffith, James E., 2003. Prediction of and effective preventative solution for annular fluid pressure buildup on subsea completed wells – case study. In: Paper SPE 84270 Presented at the SPE Annual Technical Conference and Exhibition, Denver, Colorado, 5–8 October.
- Wu, Zhiqiang, Zhou, Jianliang, Jin, Yong, et al., 2012. Difficulty analysis and technical countermeasures to the gas layer sealing ability for the shale gas horizontal well. *Oil Drill. Prod. Technol.* 34 (S1), 26–29.
- Yang, Mou, Meng, Yingfeng, Li, Gao, et al., 2013. Effects of the radial temperature gradient and axial conduction of drilling fluid on the wellbore temperature distribution. *Acta Phys. Sin.* 62 (7), 079101.
- Yin, Fei, Gao, Deli, 2014. Improved calculation of multiple annuli pressure buildup in subsea HPHT Wells. In: Paper SPE 170553 Presented at the IADC/SPE Asia Pacific Drilling Technology Conference and Exhibition, Bangkok, Thailand, 25–27 August.
- Yu, Hao, Zhanghua, Lian, Tiejun, Lin, 2014. Finite element analysis of failure mechanism of casing during shale gas fracturing. *China Pet. Mach.* 42 (8), 84–88.
- Yuan, Junliang, Deng, Jingen, Zhang, Dingyu, et al., 2013. Fracability evaluation of shale gas reservoirs. *Acta Pet. Sin.* 34 (3), 523–527.
- Zhao, Jie, Senman, Luo, Bin, Zhang, 2012. Review on Completion Fracturing Technology for Horizontal Shale Gas Well. *NGO.* 30 (1), 48–51.
- Zhou, Xianhai, 2013. Drilling & completion techniques used in shale gas horizontal wells in Jiaoshiba block of fuling area. *Pet. Drill. Tech.* 41 (5), 26–30.